NeuroResponse

Simulating Representations in the Auditory Nerve Fiber

Amaey Advait

February 2026

Neuronal Coding of Sensory Information [EC60004]

Department of Electronics and Electrical Communication Engineering

1 Introduction

Understanding how auditory stimuli are encoded by the auditory nerve fibers is a fundamental step towards modeling the auditory system. Auditory nerve fibers transform acoustic pressure signals into sequences of action potentials, which form the primary basis for the neural representation of sound. Through simulations and analyses, we aim to characterize these representations and find novel approaches to realize a practical application.

2 Part - A

Q.1

We analyze the working of the Zilany-Bruce-Carney catmodel through an experiment. *Figure(1), Figure(2)* show the tuning curves obtained from the auditory nerve fibers with best frequencies of 400Hz and 5kHz respectively. *Figure(3)* plots rate v/s intensity for both best frequencies.

Key observations:

- Each curve has a **unique peak** in the $\log_{10}(f)$ x-axis. The frequency which shows a peak at the lowest threshold/sound level is defined as the 'Characteristic Frequency' or "Best Frequency'. For the 5kHz signal, the threshold can clearly be defined as **20 dB SPL** whereas for the 400 Hz signal, no clear threshold can be identified.
- The tuning curves obtained are **asymmetric**, with a shallow slope on the low-frequency side and a steeper slope on the high-frequency side.
- The rate v/s intensity graph shows a general rise in the mean firing rate of the auditory nerve fiber with an increase in intensity. However, at lower and higher intensities, irregularities may be observed.

Q.2

In this question, we start by analyzing an audio signal. First, we truncate a snippet containing a constant vowel segment and plot the rate v/s intensity (*Figure 4*) of the snippet. Next, we shift our focus to the entire audio signal, first plotting the spectrogram of the entire waveform (*Figure 5*) and then observing the same spectrogram through the average rate as a function of time across multiple repetitions of the stimulus. (*Figure 6*).

Key observations:

- The rate v/s intensity graph(Figure 4) still shows a general rise in the mean firing rate with an increase in intensity. However, **non-differentiable points** are observed throughout the signal due to the formant frequencies changing at equal periods of time over the vowel segment, leading to specific changes in intensity.

- The spectrogram(Figure 5) shows a gradual decrease in intensity as the frequency increases. This follows from the fact that speech signals have more energy in the lower frequencies of the audible spectrum.
- We observe that as the window size increases(Figure 6), smoothness of the firing rate improves, but at the cost of temporal information.

Q.3

In this question, we simulate the phase locking phenomenon seen in auditory nerve fibers. For this, we take the fft of the Peristimulus time histogram(Psth) and filter distinct peaks by comparing the **Jensen-Shannon distance** between the primary and secondary peaks and setting a threshold for the distance to find the **dominant frequency**.

We then plot the spectrograms along two truncated best frequency banks, depicting the phase locked frequency with an asterisk (*Figure 7, Figure 8*). In both Figure 7 and Figure 8, we observe a **brightly coloured yellow band** spanning the horizontal row where the asterisk is present, which confirms that the ANF is phase locked to a dominant frequency. Here, the dominant frequency of all ANF's is **979.5819 Hz**.

Q.4

In this question, we artificially reduce the cochlear amplification factor (cohc) exponentially by setting up a threshold for the best frequency bank along with a logarithmic function. We initially see no change with respect to the normal ear, but in the phase locking spectrograms (Figures 10,11), we see that the **phase locking strength has diminished**.

Further, Figure 11 shows that the peak of the Peristimulus time histogram decreases by nearly **three-fold**. To reverse this loss in hearing, we propose a novel approach (Causal Wiener Feedback Filter, or [CWFF] in short) aimed at re-obtaining the normal ear cohc parameter from the deaf ear values.

3 Extra Credit

Causal Wiener Feedback Filter: The idea behind this approach is to combine digital signal processing and feedback techniques into one combined model that can actively improve the overall phase locking of the deaf ear. The goal is to find a methodology that can completely reverse the hearing loss caused by outer hair cell loss.

3.1 Derivation

$F(w) = |F(w)|e^{-i\phi(w)}$

Define: $H(w) = log(F(w)) = log(|F(w)|) - i\phi(w)$

Now, we split the transfer function H into even and odd components:

$H_e(w) = log_{10}(|F(w)|)$; $H_o(w) = -i\phi(w)$ [Use an adder circuit]

The even component is called the **log-amplitude spectrum**. Replacing $|F(w)|^2$ with $S_{yy}(w)$ gives:-

$H_e(w) = log_{10}(\sqrt{|F(w)|^2}) = log_{10}(\sqrt{S_{yy}})$

$H_e(w)$ *and* $H_o(w)$ are Hilbert Transform pairs. Hence,

$H_o(w) = \mathcal{H}(H_e(w)) = -i\phi(w)$

The Hilbert transform enforces causality. We now reconstruct the complex spectrum to get back S_{yyc} *and* S_{yync}

$S_{yyc} = e^{H_e(w)+iH_o(w)}$; $S_{yync} = e^{H_e(w)-iH_o(w)}$

This completes the application of Bode criterion. We find the required causal and anti-causal components and then construct the Wiener Filter:

$$\boxed{H_{wiener}(w) = \frac{q_c}{S_{yyc}} \; where \; q_c = \frac{S_{xy}}{S_{yync}}}$$

Now we return to the feedback circuit. The goal is to obtain a least squares stable solution(G) for the feedback loop.

Mathematically stated,

$$\hat{G} = \arg\min_{G} \; \mathbb{E}\|Y - GX\|_2^2$$

Hence,

$$\hat{G} = \arg\min_{G} \; \mathbb{E}[(Y - GX)^T(Y - GX)]$$

$$\hat{G} = \arg\min_{G} \; \mathbb{E}[(Y^TY - X^TG^TY - Y^TGX + X^TG^TGX]$$

$$\hat{G} = \arg\min_{G} \; \mathbb{E}[(Y^TY - 2X^TG^TY + X^TG^TGX] \text{ (transpose of a scalar)}$$

$$\hat{G} = \arg\min_{G} \; J(G) \text{ (Cost function)}$$

We now find the gradient vector of the cost function:-

$$\frac{\partial J}{\partial G} = 0$$

$$0 - 2\mathbb{E}(YX^T) + 2\mathbb{E}(XX^T)\hat{G} = 0$$

$$\boxed{\hat{G} = \mathbb{E}(YX^T)(\mathbb{E}(XX^T))^{-1}}$$

Now, $S_{yx} = \mathbb{E}(YX^T)$; $S_{xx} = \mathbb{E}(XX^T)$ (for frequency signals)

Hence,

$$\boxed{\hat{G}(w) = \frac{S_{yx}}{S_{xx}}}$$

We input this G into the closed loop equation to find H_{cl} and then use it to compute the new cohc parameter.

Thus, in this manner, we design the **Causal Wiener Feedback Filter** (CWFF).

4 Appendices

4.1 Appendix A: Figures

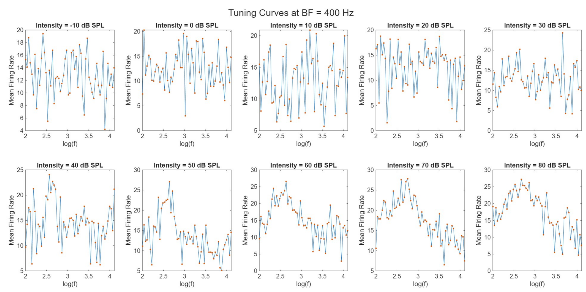

Figure 1: Tuning curves at BF = 400Hz

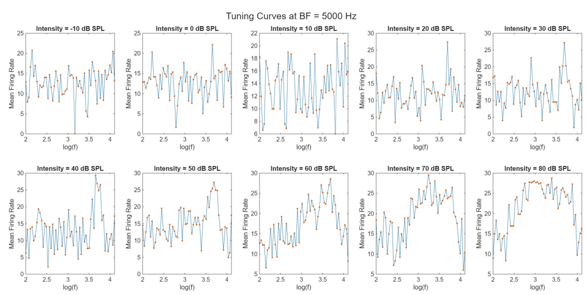

Figure 2: Tuning curves at BF = 5kHz

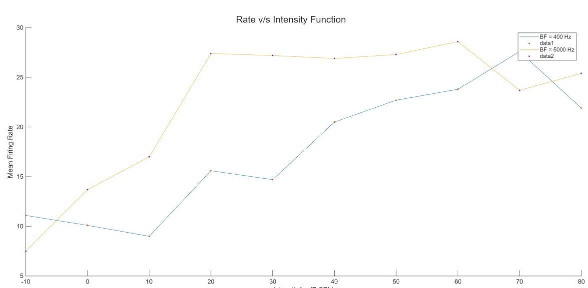

Figure 3: Rate v/s Intensity Curves for each BF

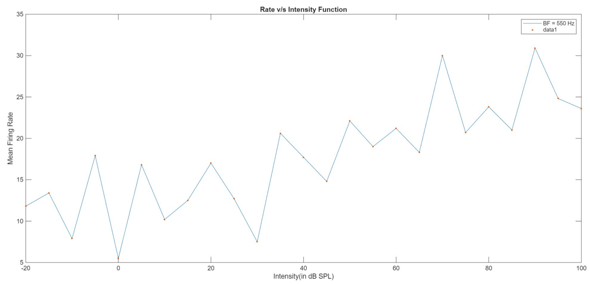

Figure 4: Rate v/s Intensity curve for BF = 550 Hz

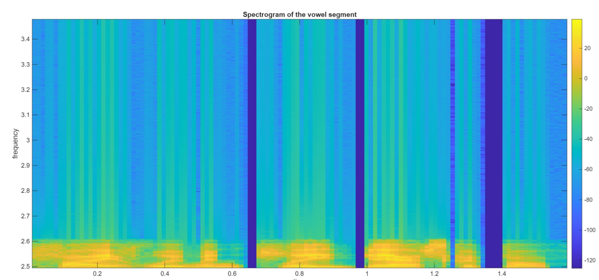

Figure 5: Spectrogram of the audio signal

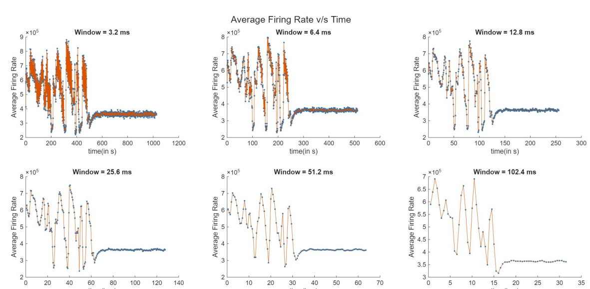

Figure 6: Firing rate v/s time curves for different windows

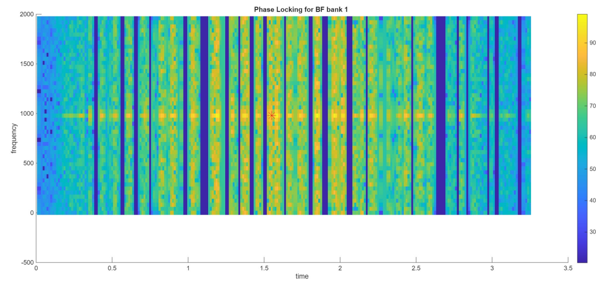

Figure 7: Phase locking spectrogram, BF bank 1, normal ear

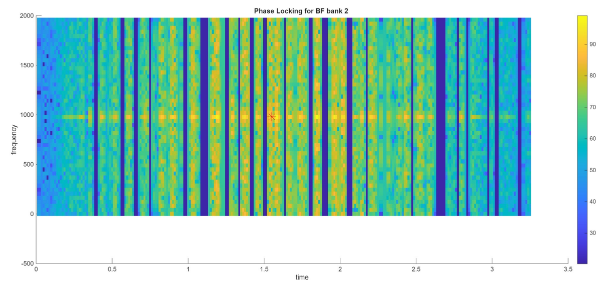

Figure 8: Phase locking spectrogram, BF bank 2, normal ear

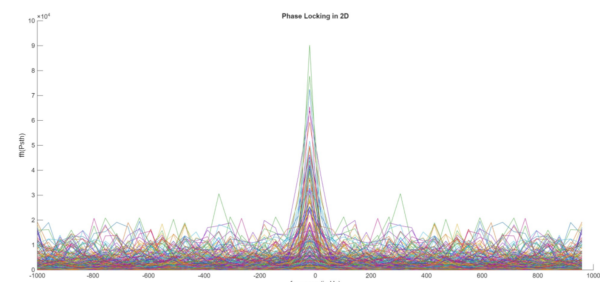

Figure 9: Phase Locking, Frequency axis, normal ear

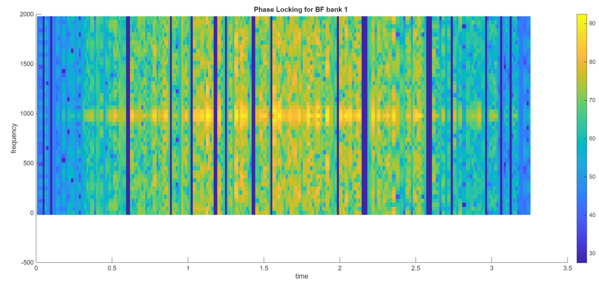

Figure 10: Phase locking spectrogram, BF bank 1, deaf ear

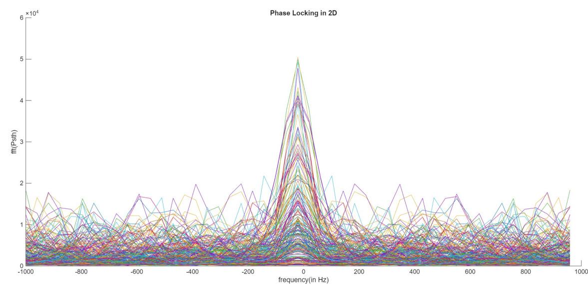

Figure 11: Phase locking, Frequency axis, deaf ear

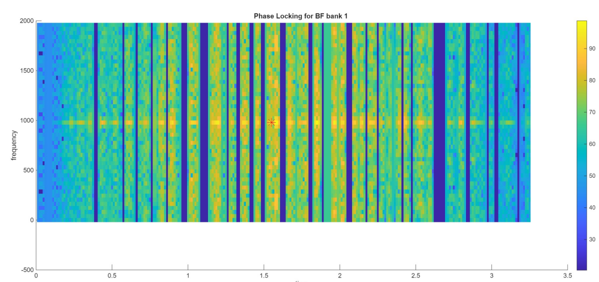

Figure 12: Phase locking spectrogram, BF bank 1, matrix inverse(I)

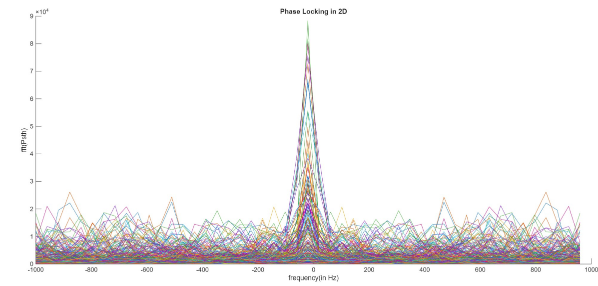

Figure 13: Phase locking, Frequency axis, matrix inverse(I)

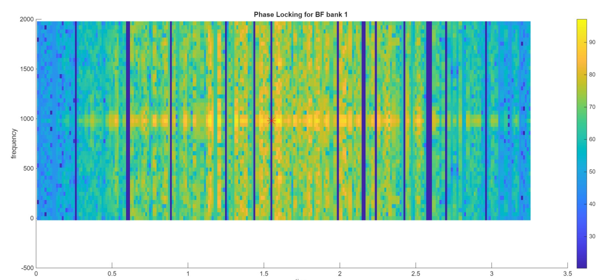

Figure 14: Phase locking spectrogram, BF bank 1, CWFF(II)

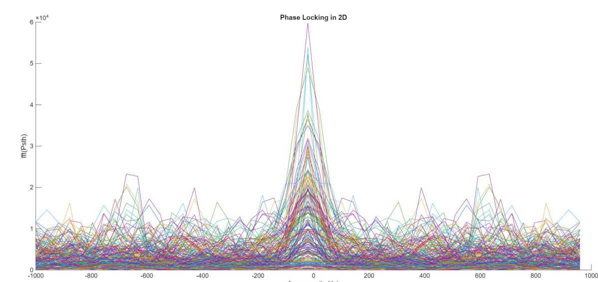

Figure 15: Phase locking spectrogram, BF bank 1, CWFF(II)

4.2 Appendix B: System-level Block Diagrams

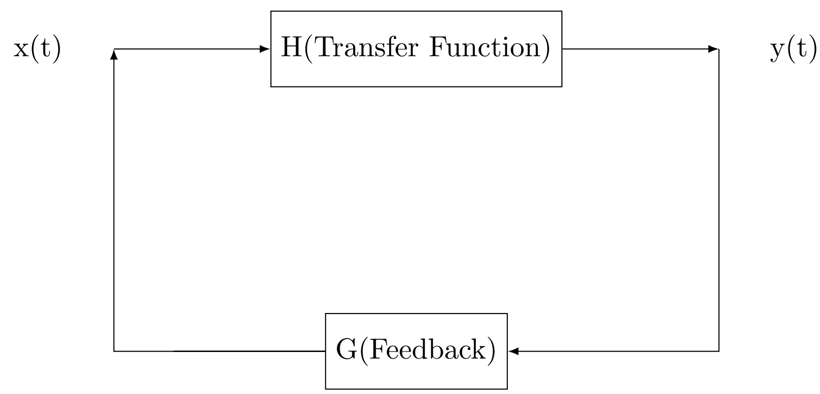

Diagram 1: High level feedback circuit representation

We draw another block diagram to give further insight into the circuit design of the transfer function.

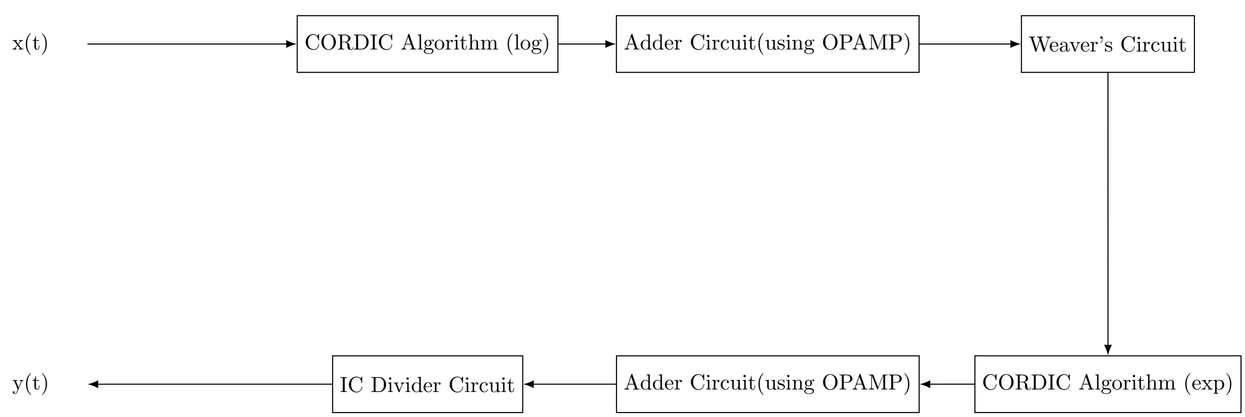

Diagram 2: Low level transfer function circuit representation

4.3 Appendix C: Limitations of the CWFF Model

The CWFF method gives a 1.5 fold selective amplification of the deaf ear's Psth while preserving phase locking(*Figure 15*). Compared to the matrix inverse solution which cannot be easily realized in hardware, a systems-level visualization of how the CWFF may be realized in a circuit is presented(Refer to *Appendix B: System-level Block Diagrams*).

However, there are several limitations of the model:-

- While CWFF can improve phase locking, damage of outer hair cells have effects on other properties as well which have not been modeled in this project.
- Wiener Filter implicitly assumes that all noise processes can be unified by passing AWGN through lumped element filters. This is a narrow way of looking at noise, which may not hold true in many scenarios in the auditory nerve fiber.
- It is computationally and electronically more energy expensive than the brain as a system.

We hope to address these limitations in the near future and shift our focus to future directions such as introducing robustness in the system towards dynamic stimuli.

5 Conclusion

In this report, we explored the neural representation of auditory stimuli through responses to tones and speech. With the help of the *Zilany-Bruce-Carney(2009)* cat model, we simulated populations of auditory nerve fibers with repeated stimuli and observed phenomena such as phase locking. We also simulated the parameters for a deaf ear and sought to engineer a solution to return the hearing of the ear to normal. As a final note, we strive to convey our continuous, active learning about the brain. Thank you for your time.